

Temperature dependence of MgB₂ Compton profiles

K. Nygård, S. Huotari, K. Hämäläinen, and S. Manninen

Division of X-Ray Physics, Department of Physical Sciences, P.O. Box 64, FIN-00014 University of Helsinki, Finland

T. Buslaps

European Synchrotron Radiation Facility, Boîte Postale 220, F-38043 Grenoble, France

N. Hari Babu, M. Kambara, and D. A. Cardwell

IRC in Superconductivity, University of Cambridge, Cambridge CB3 0HE, United Kingdom

(Received 8 August 2003; published 15 January 2004)

Changes in the momentum density of polycrystalline superconductor MgB₂ have been studied while cooling the sample below the critical temperature of 39 K. Compton-scattering experiments were performed using synchrotron radiation with incident photon energy of 29 keV at temperatures of ≈ 15 , 55, and 293 K. Small changes in the ground-state electron momentum density were observed as a function of temperature. Above the critical temperature these can be explained by thermally induced changes in the lattice constant. However, the observed localization of the valence-electron momentum density when the sample is brought into the superconducting state cannot be interpreted via thermal lattice contraction but suggests changes in the electronic structure.

DOI: 10.1103/PhysRevB.69.020501

PACS number(s): 74.25.Jb, 78.70.Ck

I. INTRODUCTION

The recent discovery of superconductivity below 39 K in MgB₂ (Ref. 1) has generated a considerable amount of interest in the material and its electronic properties,² especially concerning the nature of the observed superconductivity. The unit cell of hexagonal MgB₂ consists of one magnesium and two boron atoms containing only 22 electrons. This is significantly lower than in the structurally and chemically simplest high- T_c oxide superconductor, doped La₂CuO₄, which contains more than 150 electrons in the unit cell.

The mechanism of superconductivity in MgB₂ seems to be consistent with the conventional phonon-mediated theory.^{3–5} Computational^{6–8} and experimental^{9–12} analysis on MgB₂ further indicates anisotropic phonon-electron coupling and multigap structure as well as the importance of the two-dimensional boron σ (sp_xp_y) bands for superconductivity in the material. There are also experimental observations of electron transfer from the boron π (p_z) bands to the boron σ bands, in the transition from the normal state at room temperature to the superconducting state at 15 K.¹³ However, in order to understand the mechanism of superconductivity in MgB₂, more experimental and computational information is needed about the electronic structure and the properties of the material, both in the normal and the superconducting state.

Compton scattering, i.e., inelastic x-ray scattering from electrons at large energy and momentum transfers, is a unique tool for studying ground-state electron momentum densities.^{14,15} Compton scattering is neither sensitive to crystal defects nor to surface effects. Modern third-generation synchrotron-radiation facilities allow experiments with both good momentum resolution and high statistical accuracy. Hence the technique has been frequently used for studying ground-state electronic properties of matter.

In a Compton-scattering experiment the double-

differential cross section is measured. For a review on Compton-scattering theory, see, e.g., Ref. 16. Within the impulse approximation the cross section can be written¹⁷

$$\frac{d^2\sigma}{d\Omega d\omega_2} = C(\omega_1, \omega_2, \phi) J(p_z). \quad (1)$$

Hence the cross section is factorized into a part which depends only on the experimental setup, $C(\omega_1, \omega_2, \phi)$, and a part which carries information on the ground-state properties of the electronic system, known as the Compton profile $J(p_z)$. The Compton profile is defined by the initial electron momentum density $N(\mathbf{p})$ through a two-dimensional integral in a plane perpendicular to the scattering vector

$$J(p_z) = \iint dp_x dp_y N(\mathbf{p}). \quad (2)$$

In other words, the Compton profile is a one-dimensional projection of the integrated electron momentum density along the direction of the scattering vector. By using the definition of the electron momentum density

$$N(\mathbf{p}) = \sum_{\nu} \left| \int d^3\mathbf{r} \psi_{\nu}(\mathbf{r}) e^{i\mathbf{p}\cdot\mathbf{r}} \right|^2, \quad (3)$$

where ν denotes the band index and the summation is over the occupied states, it is clear that the Compton profile is normalized to the number of electrons in the unit cell of the sample,

$$\int_{-\infty}^{\infty} dp_z J(p_z) = N \text{ electrons}. \quad (4)$$

Since the Compton profile is defined in the momentum space, the technique is more sensitive to the valence than to the core electrons. This is due to the fact that the valence

electrons, unlike the core electrons, are localized in momentum space, leading to a narrow contribution to the Compton profile.

In the case of superconductivity the electrons of interest are the valence electrons close to the Fermi surface. In MgB_2 the ratio of the number of these electrons and the total number of electrons in the unit cell is rather large, when compared to, e.g., high- T_c oxide superconductors. Hence one expects that any change in the electronic structure connected to the transition from normal to superconducting state would be easier to detect in MgB_2 than in the case of high- T_c superconductors. For the latter case no change in the Compton profile has been observed in the superconducting phase transition.¹⁸

This paper reports a temperature-dependent Compton-scattering study on polycrystalline MgB_2 . This is motivated by the need of experimental work on the electronic structure and properties in both normal and superconducting states. Three sets of Compton-scattering measurements were carried out at temperatures of ≈ 15 , 55, and 293 K using an incident photon energy of 29 keV. In the experiments we used two different spectrometers simultaneously, a high- and a low-resolution spectrometer with momentum resolutions of ≈ 0.10 and 1.1 atomic units (a.u.), respectively.

II. EXPERIMENT

The experiment was performed at beam line ID15B at the European Synchrotron Radiation Facility. The radiation was produced by an asymmetric multipole wiggler and monochromatized using a horizontally bent Si crystal utilizing the (111) reflection. The Compton profiles were measured at temperatures of 15, 55, and 293 K. The data were collected simultaneously using a scanning Rowland circle spectrometer with a cylindrically bent Si(400) analyzer crystal at a scattering angle of $\phi \approx 173^\circ$ and an intrinsic Ge solid-state detector, which was positioned to measure the scattered radiation at an angle of $\phi \approx 148^\circ$. Details about the spectrometer can be found in Ref. 19. The raw data acquired by the scanning-crystal spectrometer were normalized using the solid-state detector data and corrected for absorption in the sample and in the path of the scattered radiation as well as for the analyzer reflectivity. The energy spectra acquired by the Ge detector were corrected only for the absorption in the sample and in the path of the scattered radiation.

Cylindrical pellets (16 mm of diameter and 5 mm thick) were prepared from a mixture of high-purity Mg and B powders ball milled under argon using an evacuated press die set to minimize the air trapped in the sample. The pellet was sandwiched between $\text{Mo}/\text{Al}_2\text{O}_3$ plates and placed in an alumina crucible. Pure Mg powder was placed close to the sample to suppress the oxidation and evaporation of Mg from the sample during densification. The pellets were heat treated in a Mg-coated tube furnace under an applied load of 10 N at 850 °C under flowing 4% $\text{H}_2 + \text{Ar}$ gas for 10 h. X-ray-diffraction analysis confirmed the sample to be single phase and MgO-free MgB_2 . Microstructural investigations confirmed the sample to be polycrystalline with a grain size of several tens of microns in diameter. Full details of sample

preparation are given in Ref. 20. Finally such a pellet was cut to a size of $12 \times 4 \times 1.5 \text{ mm}^3$.

The sample was cooled using a closed-cycle cryostat with a temperature controller, utilizing pressurized He gas of 16 bars. A Cu sample holder was mounted on the cold finger. The cold finger, sample holder, and sample were in a vacuum chamber and all the experiments were performed in vacuum. The temperature of the sample was monitored using two thermal monitors, a Cernox thermal sensor (control sensor) at the base of the cold finger, and a PT-100 resistor (monitor sensor) mounted directly on the tip of the sample. However, since the PT-100 resistor levels off at $T = 23.15 \text{ K}$, we had to rely solely on the Cernox sensor below this temperature. Concerning the measurements at the lowest temperature, where the control sensor reading was 12 K, we know nevertheless that we were well below 23.15 K. Furthermore, according to earlier calibration measurements the temperature was expected to be $\approx 15 \text{ K}$. The thermal conductivity between the sample and the temperature sensor as well as the sample holder and the sample was enhanced using conductive grease (Lakeshore Cry-Con). The consistency between the two temperature monitors was good, the difference in the readings of the sensors above 23.15 K was measured to be less than 1 K. This difference was due to the radiative heating of the sample and finite thermal conductivity of the sample holder and the sample.

The total momentum resolution of the scanning-crystal spectrometer was $\Delta p_z \approx 0.10 \text{ a.u.}$ At the Compton peak a total of 7.5×10^5 counts were collected at each temperature and hence the statistical inaccuracy was about 0.1%. The total momentum resolution of the Ge solid-state detector was $\Delta p_z \approx 1.1 \text{ a.u.}$ The momentum resolution of the Ge spectrometer was dominated completely by the energy resolution of the detector, which was close to 400 eV at the Compton peak. With this detector, at the Compton peak a total of 6.8×10^6 ($T = 15 \text{ K}$), 1.6×10^7 ($T = 55 \text{ K}$), and 6.2×10^6 ($T = 293 \text{ K}$) counts were collected resulting in a statistical inaccuracy of about 0.04%, 0.03%, and 0.04%, respectively. The excellent statistical accuracy is naturally the motivation for using the low-resolution spectrometer in the first place.

During the experiment, the spectra were measured repeatedly several times and added together using the associated statistical accuracy as a weight. This assured the monitoring of the nonstatistical fluctuations as well, which can be significant when the statistical accuracy is this high. The difference between each spectrum and the sum of the spectra were found to be within the statistical uncertainty in all cases. The background, which was linear in the energy scale, was subtracted from the data by assuming the high-momentum tails of the Compton profiles to be due to the core electrons. The background was as low as 0.1% of $J(0)$ for both the scanning-crystal spectrometer and the Ge detector data.

The measured scattering cross sections were further corrected for relativistic effects according to Holm,²¹ converted to the momentum scale, and the negative and positive momentum sides of the profiles were averaged since the Compton profiles are intrinsically symmetric. Finally the profiles were normalized to the number of electrons.

A very important property of MgB_2 concerning our ex-

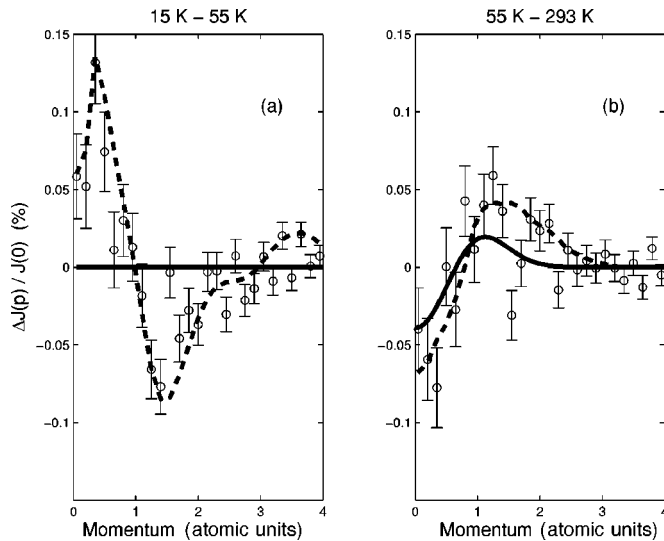


FIG. 1. Differences in the experimental Compton profiles acquired at temperatures of (a) 15 K and 55 K and (b) 55 K and 293 K using the solid-state detector ($\Delta p_z \approx 1.1$ a.u.). The thick solid lines are the corresponding differences given by a free-electron model while the dashed lines are merely a guide for the eye.

periments is the temperature dependence of the lattice parameters. Since the change in the Compton profile in the transition from the normal to the superconducting state is expected to be small, it is crucial that the changes in the lattice parameters are small or at least well known. Fortunately, for MgB_2 there is practically no change in the lattice parameters when the temperature is below 70 K.²² Thus changes in the electronic structure and the related wave functions are not notably distorted by the lattice effects in the vicinity of the critical temperature.

III. RESULTS AND DISCUSSION

The main results of the experiment are given in Figs. 1 and 2, where the temperature-dependent differences of the symmetrized Compton profiles are plotted. Figure 1 shows the difference between the Compton profiles acquired using the solid-state detector ($\Delta p_z \approx 1.1$ a.u.) and Fig. 2 the difference found using the scanning-crystal spectrometer ($\Delta p_z \approx 0.10$ a.u.). In both figures, the left-hand side subplot (a) is based on the data acquired at temperatures of 15 and 55 K and the right-hand side subplot (b) at temperatures of 55 and 293 K, respectively ($T_C = 39$ K). The error bars represent the magnitude of the statistical inaccuracy while the dashed lines are guidelines for the eye. Finally, the thick solid lines represent a theory where the valence electrons are treated within the free-electron model and convoluted with the corresponding experimental resolution function. In this model one takes into account only the thermal expansion of the real-space lattice, i.e., shrinking of the reciprocal lattice, as the temperature increases. The corresponding change of the Fermi momentum leads to a narrower Compton profile, since the states are confined to smaller momentum values at higher temperatures. It should be mentioned that the results of this rather simple free-electron model above the critical tempera-

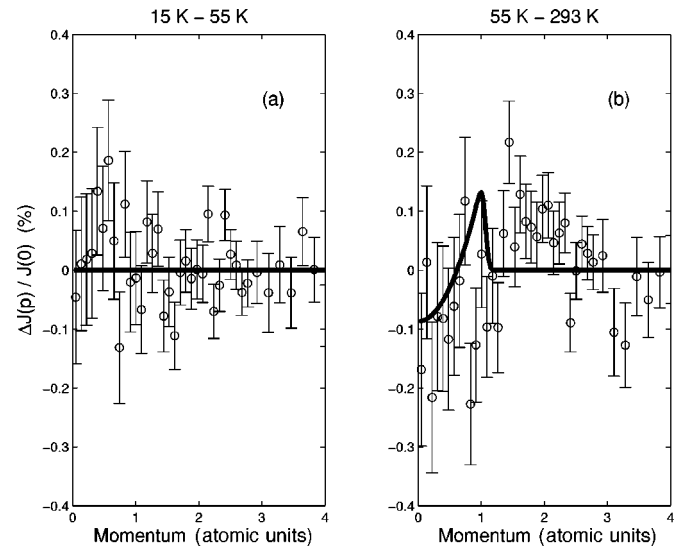


FIG. 2. As for Fig. 1, except that the data are acquired using the scanning-crystal spectrometer ($\Delta p_z \approx 0.10$ a.u.).

ture are in good qualitative agreement with an *ab initio* calculation.²³

The changes in the Compton profiles as a function of temperature above T_C are shown in the subplots (b) of Figs. 1 and 2. As can be seen from Fig. 1(b), the general behavior is rather well explained by the free-electron model. However, with the moderate momentum resolution of the solid-state detector, we cannot extract any fine structure from the data. Figure 2(b), showing similar data but acquired with the scanning-crystal spectrometer, reveals a change in the experimental Compton profile extending to momentum $p_z \approx 3$ a.u., which cannot be explained by the free-electron model prediction. The qualitative similarity between Figs. 1(b) and 2(b) rules out the possibility that this is due to an experimental artifact. It could possibly be due to contributions of higher Brillouin zones. However, considering the relatively high Debye temperature ($\Theta_D \approx 800$ K) of MgB_2 ,² these effects should be relatively small. Thus further theoretical studies, similar to those done for Be,²⁴ are needed to explain the behavior in Fig. 2(b). It should be noted that the changes in the Compton profiles are extremely small, only about $\pm 0.1\%$ of $J(0)$. This is of the same order as the statistical accuracy of the scanning-crystal spectrometer and thus close to the experimental detection limit.

The changes in the Compton profiles in the transition from normal to superconducting state are shown in subplots (a) of Figs. 1 and 2. In this case there should be no difference in the Compton profiles due to thermal expansion, as indicated by the results of the free-electron model. Yet, in the data acquired using the solid-state detector, we observe a localization of the valence-electron momentum density when comparing the profiles acquired at temperatures of 55 K and 15 K. Here the statistical accuracy of the scanning-crystal spectrometer is not sufficient to indicate whether the width of the experimental curve in Fig. 1(a) is intrinsic or limited by the detector resolution.

As far as we know, there is no simple theory which explains the observed changes in the Compton profiles ac-

quired in the normal and the superconducting states. It is possible that Cooper pairing²⁵ leads to a localization of electron density in momentum space. However, in order to relate this phenomenon to our experimental results one would need to develop a theoretical approach, which includes this cooperative phenomenon.

As mentioned in the Introduction, there have been observations of electron transfer from the p_z to the $p_x p_y$ bands during the transition from normal state at room temperature to the superconducting state at 15 K. How and to what extent this observed electron transfer would modify the Compton profile is not yet known. High-resolution Compton-scattering measurements on single-crystalline samples could provide an

insight into this effect, although samples of sufficient size are not yet available. Furthermore, development work on more sophisticated cluster calculations to model the charge transfer within boron rings to address this specific issue are currently in progress.

ACKNOWLEDGMENTS

We would like to acknowledge A. Bansil for discussions and comparison of our model with their preliminary calculations on MgB₂. This work was supported by the Academy of Finland under Grant Nos. 50584, 74440, and 210291.

-
- ¹J. Nagamatsu, N. Nakagawa, T. Muranaka, Y. Zenitani, and J. Akimitsu, *Nature (London)* **410**, 63 (2001).
- ²For a review see, e.g., C. Buzea and T. Yamashita, *Supercond. Sci. Technol.* **14**, R115 (2001).
- ³J. Bardeen, L.N. Cooper, and J.R. Schrieffer, *Phys. Rev.* **106**, 162 (1957); **108**, 1175 (1957).
- ⁴G.M. Eliashberg, *Zh. Eksp. Teor. Fiz.* **38**, 966 (1960) [*Sov. Phys. JETP* **11**, 696 (1960)].
- ⁵W.L. McMillan, *Phys. Rev.* **167**, 331 (1968).
- ⁶P.P. Singh, *Phys. Rev. Lett.* **87**, 087004 (2001).
- ⁷A.Y. Liu, I.I. Mazin, and J. Kortus, *Phys. Rev. Lett.* **87**, 087005 (2001).
- ⁸N.V. Dobrodey, A.I. Streltsov, L.S. Cederbaum, C. Villani, and F. Tarantelli, *Phys. Rev. B* **66**, 165103 (2002).
- ⁹M. Iavarone, G. Karapetrov, A.E. Koshelev, W.K. Kwok, G.W. Crabtree, D.G. Hinks, W.N. Kang, E.-M. Choi, H.J. Kim, H.-J. Kim, and S.I. Lee, *Phys. Rev. Lett.* **89**, 187002 (2002).
- ¹⁰H. Uchiyama, K.M. Shen, S. Lee, A. Damascelli, D.H. Lu, D.L. Feng, Z.-X. Shen, and S. Tajima, *Phys. Rev. Lett.* **88**, 157002 (2002).
- ¹¹Y. Zhu, A.R. Moodenbaugh, G. Schneider, J.W. Davenport, T. Vogt, Q. Li, G. Gu, D.A. Fischer, and J. Taftø, *Phys. Rev. Lett.* **88**, 247002 (2002).
- ¹²E.Z. Kurmaev, I.I. Lyakhovskaya, J. Kortus, A. Moewes, N. Miyata, M. Demeter, M. Neumann, M. Yanagihara, M. Watanabe, T. Muranaka, and J. Akimitsu, *Phys. Rev. B* **65**, 134509 (2002).
- ¹³E. Nishibori, M. Takata, M. Sakata, H. Tanaka, T. Muranaka, and J. Akimitsu, *J. Phys. Soc. Jpn.* **70**, 2252 (2001).
- ¹⁴M.J. Cooper, *Radiat. Phys. Chem.* **50**, 63 (1997).
- ¹⁵S. Manninen, *J. Phys. Chem. Solids* **61**, 335 (2000).
- ¹⁶M.J. Cooper, *Rep. Prog. Phys.* **48**, 415 (1985).
- ¹⁷P. Eisenberger and P.M. Platzman, *Phys. Rev. B* **2**, 415 (1970).
- ¹⁸S. Manninen, K. Hämäläinen, M.A.G. Dixon, M.J. Cooper, D.A. Cardwell, and T. Buslaps, *Physica C* **314**, 19 (1999).
- ¹⁹P. Suortti, T. Buslaps, P. Fajardo, V. Honkimäki, M. Kretzschmer, U. Lienert, J.E. McCarthy, M. Renier, A. Shukla, T. Tschentscher, and T. Meinander, *J. Synchrotron Radiat.* **6**, 69 (1999).
- ²⁰M. Kambara, N. Hari Babu, E.S. Sadki, J.R. Cooper, H. Minami, D.A. Cardwell, A.M. Campbell, and I.H. Inoue, *Supercond. Sci. Technol.* **14**, L5 (2001).
- ²¹P. Holm, *Phys. Rev. A* **37**, 3706 (1988).
- ²²J.D. Jorgensen, D.G. Hinks, and S. Short, *Phys. Rev. B* **63**, 224522 (2001).
- ²³A. Bansil *et al.* (unpublished).
- ²⁴S. Huotari, K. Hämäläinen, S. Manninen, C. Sternemann, A. Kaprolat, W. Schülke, and T. Buslaps, *Phys. Rev. B* **66**, 085104 (2002).
- ²⁵L.N. Cooper, *Phys. Rev.* **104**, 1189 (1956).